.

UV Image Sensors and Associated Technologies

Charles L. Joseph

Space Astronomy Laboratory
University of Wisconsin
1150 University Ave.
Madison, Wisconsin 53706
clj@alberio.astro.wisc.edu

An Invited Review for Experimental Astrophysics

Abstract

Large-format ultraviolet image sensors have been and are actively being developed for a variety of space-borne astronomy missions. The detector, which historically is one of the most problematic parts of any astronomical spacecraft, plays a critical role in the overall capability of the instrument. There are numerous detector systems with none being ideal for all applications. This paper presents an overview of UV image sensors that are currently available and associated technologies that are undergoing further development. Special attention is given to physical processes responsible for the inherent strengths and weaknesses of a few important UV detectors. Technological advances that are likely to impact the performance of future image sensors are also discussed.

1 Overview

Although the detector typically accounts for only a small fraction of the total expenditure on hardware, frequently it is the limiting item affecting the overall data quality and for a telescope of a given aperture, it determines the feasibility of the various science projects. Furthermore, the detector historically has been one of the most problematic elements in any instrument. Hence, this important component deserves particular attention.

The ultraviolet spectrum extends from wavelengths of approximately 70 to 3000 Å. For practical reasons, this interval shall be divided into four parts based on the appropriate technologies. For example, most detectors are configured with windows for use above 1216 Å, but for windowless operation below this wavelength since transmission efficiencies are extremely poor. (Note that in this context windows or faceplates are used to form a sealed, stand-alone image sensor which is simpler to test and protects internal parts against contamination.) While each wavelength regime has its own particular set of detector requirements, one cannot ignore relevant technologies that are being developed for observations ranging from X-rays to optical photons. Note that various scientific communities use different nomenclature to describe individual wavelength bands. The main emphasis of the present review shall be on detectors operating in the 912 to 1216 Å and especially in the 1216 to 2000 Å wavelength ranges, which shall be referred to as the FUV (Far UV) and UV respectively. The adjacent wavelength bands 70 to 900 Å and 2000 to 3000 Å shall be referred to as the EUV (Extreme UV) and Near UV, respectively.

In some circumstances, specialized missions have fewer detector requirements than instruments designed for a broad range of applications. Occasionally, these missions can take advantage of a unique strength of a particular detector system that otherwise might not be as universally competitive. The science drivers, however, require a general-purpose UV image sensor to have 5 primary properties above all else: 1) it should NOT be sensitive to light at optical wavelengths (commonly referred to as being solar blind), 2) it should have high Detective Quantum Efficiency (DQE), 3) it should have a high Local Dynamic Range (LDR), 4) it should have low backgrounds since noise arising from the background often dominates in faint UV observations and 5) it should have a large multiplexing capability (i.e. a large number of pixels) to maintain sufficient field of view or to record significant amounts of spectra simultaneously. Obviously, there are several other important parameters, but these are normally achieved with most detector systems and therefore are of less concern.

For many observations, the source itself produces more flux at optical wavelengths than it does in the UV. Astronomical objects often emit 10^4 to 10^8 visible photons for every UV photon in the 1000 to 2000Å wavelength region. If the detector also has its maximum sensitivity at these longer wavelengths then the data will contain an enormous background contribution that substantially increases the noise. This statement is valid even if a UV filter is used, which typically has a 10^{-3} to 10^{-4} transmission at optical wavelengths. DQE is is taken to mean the final product (i.e. the total signal accumulation efficiency). DQE incorporates all losses including, for example, those due to the transmission efficiency of a

window or the conversion efficiency of the electronics neither of which is ever perfect. A Charge Coupled Device (CCD) for instance may have a QE of 20 percent in the UV, but if it must be placed behind an Alkali metal filter (Woods filter) to make it solar blind, its ultraviolet DQE will typically be only 1-4%.

LDR is defined as the maximum level of flux that can be accommodated in a small area of the detector minus the faintest level that is still 3 standard deviations above the background for practical integration times. Note that most UV astronomical scenes have most of the light in a relatively few pixels or are generally faint so that the Global Dynamic Range (GDR), the total flux rate spread over the whole detector, is rarely important for imaging applications. GDR is important nevertheless for echelle spectra of bright hot stars or for observing the sun. Similarly, the GDR determines the time required to accumulate a calibration flat field to measure the pixel-to-pixel sensitivity.

Contributions to the background include internal detector darks and externally induced sources. For example, cosmic rays interacting with MgF_2 faceplates used in image tubes can in some circumstances produce measurable amounts Cherenkov radiation. The integration times of individual CCD frames is usually set by the levels of cosmic ray hits that are tolerable. The backgrounds of most detectors are thus sensitive to their environment (i.e. whether or not the sensor is in the South Atlantic Anomaly or above or below the Van Allen Radiation Belt).

In general, image sensors can be broken down into several classes. Two typical classes, Photoconductive and Photoemissive, are represented schematically in Figure 1, which also demonstrates some of the inherent properties of each. A wavelength scale with corresponding photon energies and thermal equivalences are shown at the bottom. Photoconductive devices, which absorb the photons into the semiconductor substrate, have sensitivities over a broad range of wavelengths while photoemissive detectors use various photocathodes that are tailored to be sensitive to a specific, limited-wavelength interval.

In photoconductive devices, the photon causes an electron to transition into the conduction band. The most common photoconductive devices are silicon-based CCDs where the detection process requires energies of approximately an electron volt. It is readily apparent from Figure 1 that photoconductive devices should (and do) have excellent sensitivity in the optical and near-IR portion of the electromagnetic spectrum and that these devices should be sensitive to thermally-induced backgrounds at room temperatures. Note: the photodetection process is only efficient if the photon energies are somewhat above the minimum activation energy.
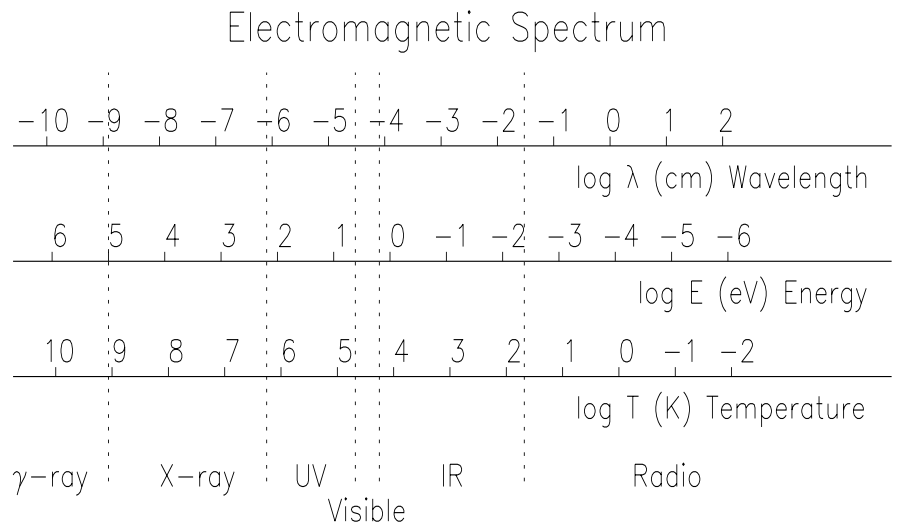
Image Sensors

Photoelectric

Photographic

Photoconductive

~1 eV => Optical λs
      => Therm. Bg

Examples: CCD, CID

Photoemissive

several eV => UV λs
          => No Cooling Needed

Examples: MCP, EBCCD, Vidicon

Electromagnetic Spectrum

−10 −9 −8 −7 −6 −5 −4 −3 −2 −1 0 1 2

log λ (cm) Wavelength

6 5 4 3 2 1 0 −1 −2 −3 −4 −5 −6

log E (eV) Energy

10 9 8 7 6 5 4 3 2 1 0 −1 −2

log T (K) Temperature

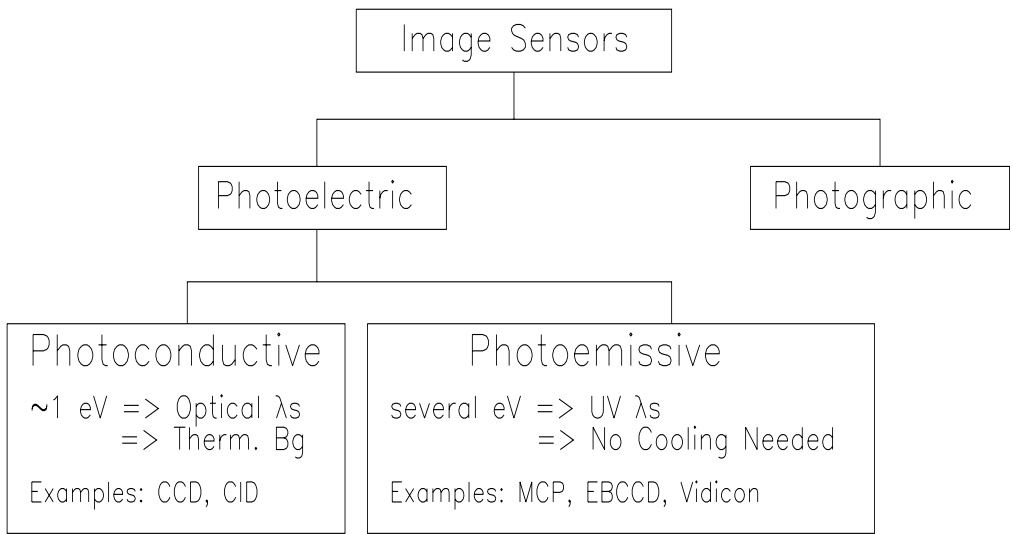γ−ray   X−ray   UV   IR   Radio

Visible

Fig. 1 showing schematically two classes of photoelectric detectors:
photoconductive and photoemissive. As is readily evident, photoconductive
devices are inherently good optical detectors having thermal backgrounds,
while photoemissive devices are natural in the UV. Note, however, that
there is some overlap between these two classes (see text for details).

In contrast, the photon in photoemissive devices must have sufficient energy to eject an
electron from a photocathode material, typically requiring energies of a few electron volts.
These image sensors are therefore natural UV detectors that produce negligible dark back-
grounds at room temperatures. Photoemissive devices can be constructed to be inherently

4

solar blind as well. A single photoelectron, however, cannot be recorded reliably without some form of intensification, which implies high voltages and the inherent associated difficulties. If the intensification process is saturated and has sufficient gain, detectors that are photon counting with zero read noise can be constructed. Although photoconductive devices such as the CCD are not photon counting at UV or optical wavelengths, researchers have had great success in reducing the read noise to the point where the signal-to-noise ratios achieved with these devices become competitive with photon-counting detectors except at very low flux levels or except where very high time resolution is required.

Obviously there is some overlap between various classes of detectors. For example, photoemissive devices with photocathodes such as the S20 have been developed with response well into the visual. Detectors with S20 photocathodes do have to be cooled to reduce the dark counts. Similarly, solid-state scientists are experimenting with GaAlN, diamond and various other substrates with large band gaps between the valence and conduction bands. Photoconductive detectors made from these materials have the potential to be inherently superior UV sensors than current CCDs.

There are far too many different UV detector systems to give adequate coverage to each. For example, the Precision Analog Photon Address (PAPA) is one ingenious photon-counting detector based on 9 + 9 photomultiplier tubes capable of encoding 512×512 pixels (Papalios & Mertz 1982; Gonsiorowski 1986). This device is not in the mainstream of current design and has been omitted from the present discussion. Since no single detector system is uniquely well suited for all applications, this review attempts to highlight the advantages and disadvantages of a few key UV image sensors that have or will soon have significant impact on ultraviolet astronomical observations. As already stated, the present review emphasizes the UV and FUV with special attention being paid to technological advances needed to overcome existing physical limitations. These advances have and will continue to come from technologies being developed for observations spanning a much broader range of wavelengths. An extensive examination of various detector systems for both imaging and nonimaging applications is presented by Carruthers (1993). Reviews of detectors for optical wavelengths have been presented by Timothy (1983) and for a comparison of CCDs to other optical detectors by Janesick *et al.* (1984). In addition, the reader is referred to an excellent book entitled: "Low light level detectors in astronomy" by Eccles, Sim, & Tritton (1983). X-ray detectors have been reviewed by Ramsey, Austin, and Decher (1994) as well as in a comprehensive text entitled: "Detectors in X-Ray Astronomy" by Fraser (1989). A previous review of UV detectors specifically is given by Timothy and Madden (1983), while a similar review of detectors suitable for the EUV was given by Lampton (1991). Photon counting detectors which dominate UV/FUV/EUV sensor technology have been reviewed by Timothy (1991a) and the important subset based on the microchannel plate have been reviewed by Timothy (1985) and by Siegmund *et al.* (1992). NASA's short- and long- term requirements for new UV sensors and the corresponding new technologies for the 21st century can be found in a technology development study led by the Jet Propulsion Laboratory called Astrotech 21 (B. Wilson, ed. 1991) as well as in Welsh (1992).

2   Existing Technologies

2.1   A Brief Comparative Assessment

A few detector systems are discussed in much greater detail in the remaining subsections. For clarity, this subsection provides a brief comparison of performances of existing technologies with a minimal discussion of the physical processes leading to the various limitations.

As already noted, the photoemissive detectors are inherently good UV, FUV and EUV detectors. This class of device can be further broken down into various types, some examples of which are given in Figure 1. One of the most successful types of ultraviolet detector is that based on the microchannel plate (MCP). Detector systems using MCPs have been and will be used in numerous instruments for X Ray Observations (see Fraser, Barstow, and Pearson 1988 and references therein; Murray and Chappell 1988), for Extreme Ultraviolet Missions (Malina *et al.* 1982, Siegmund *et al.* 1989) and for the FUV/UV ($\lambda > 900$ Å, e.g. Davidsen *et al.* 1992; Hurwitz & Bowyer 1991). Future NASA UV/Visible missions using an MCP-based detector include reflights of ORFEUS/IMAPS and ASTRO-2 as well as major new instruments such as SOHO, CASSINI, STIS, and FUSE. Furthermore, MCPs are being used as image intensifiers for CCDs as well as for Reticons.
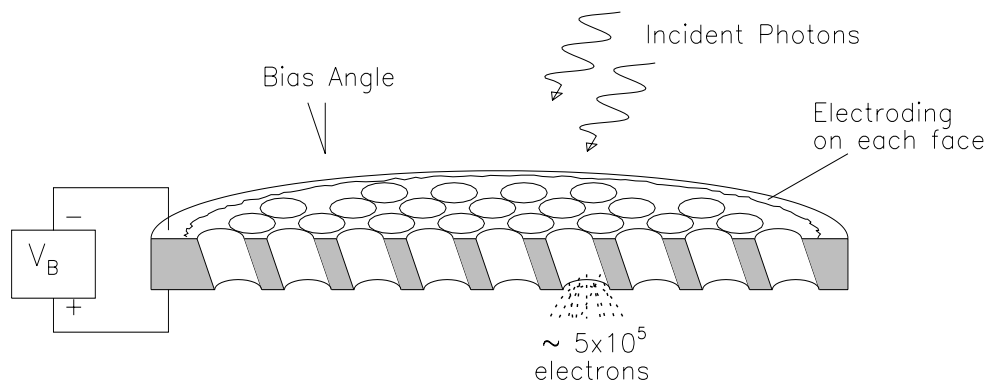

Fig. 2 a schematic drawing of a Microchannel Plate (MCP) showing half of the plate. The ratio of pore length to pore diameter (L/D) range typically from 40:1 to 120:1.

An MCP essentially is a small, thin disk of lead-oxide glass with numerous microscopic channels, running parallel to each other from one face of the disk to the other. A schematic cross section of an MCP is pictured in Figure 2. When an electric potential is applied between the two faces, the MCP becomes an image intensifier. The device can be considered to be a compact assemblage of photomultipliers since electrons striking the walls of a pore

liberate additional electrons in a continuous dynode fashion to produce an avalanche. If the potential is sufficiently large, a photoelectron then gives rise to a saturated electron cloud with a total charge falling within a narrow range that can be easily "counted" electronically. Unfortunately, MCPs have a significant surface-to-volume ratio which readily traps residual gas. Cleanliness and plate conditioning are thus important issues since MCPs are normally operated at potentials in excess of 1KeV which can cause destructive discharges.

Plates with active areas as large as 100×100 mm^2 are common. MCP channels typically are 8-25 μm in diameter and are on 10-40 μm centers. Pulses emerging from the bottom of a single MCP pore typically have 10^4 to 10^6 electrons. A photocathode material can be placed on the top face of the MCP or on a window in proximity focus just above the MCP. Various anode structures, which will be discussed in the next section, or a solid state device can be placed below the MCP to encode the event location.

Photon-counting MCP detectors, which are inherently solar blind, currently have a significant DQE advantage over charge coupled devices (CCDs) at wavelengths shortward of 2000 Å, but lack the dynamic range of a large-pixel CCD. Also for applications not requiring solar blindness, CCDs offer the potential for higher sensitivity over image tubes. For these reasons, there is considerable interest in developing technologies to enhance the CCD's sensitivity to UV radiation. Another obvious advantage of the photoconductive devices such as the CCD is the direct detection of UV, EUV or even X-ray radiation, rather than having to rely on some form of intensification and its associated difficulties. This makes this type of image sensor lighter, smaller, and less complex than most photoemissive devices and it does not require any high voltages which are always a reliability risk. Furthermore, a CCD does not have a QE that is a strong function of the angle of incidence of the photons as do all MCP-based detectors.

While it is possible that technological advances in the next few years will take the solar-blind DQEs of CCDs from the current 1-5% to the 10-20% routinely obtained with MCP-based detectors, there are 3 difficult technological problems to overcome and all three must be achieved simultaneously! These are discussed in §2.3. The technologies required to make CCD-based detectors competitive for wavelengths below 2000 Angstroms are formidable, especially for pixel sizes below 15 microns where the dynamic range advantage is diminished. It should be noted that while CCDs currently do not have high solar-blind DQEs in the UV, CCDs can and are used successfully in certain detector systems where an intensification method is used. An MCP-Intensified CCD (ICCD) is one example.

Detectors such as the ICCD in Figure 3 require multiple conversions between light and electronic signals, each producing some degradation. While the ICCD, operated in photon-counting mode in which individual intensified photoevents are centroided, can provide impressive spatial resolution, the framing rate of the CCD and phosphor decay effects impose severe constraints on the Local Dynamic Range. Although investigators have introduced frame-to-frame comparisons (subtractions) in an attempt to mitigate the phosphor's persistence, the algorithms are cumbersome, often requiring 8 or more previous frames, and even then are only partially successful (Jenkins 1994 - private communication). Rarely

7

have LDRs greater than 5 counts/pixel/second been possible. For many EUV applications having low flux levels, a low LDR is not a serious limitation. EUV sensors similar in design to Figure 3 but that are mosaics have been fabricated (e.g. Williams and Weistrop 1983, Roberts, Tuohy, & Dopita 1988).
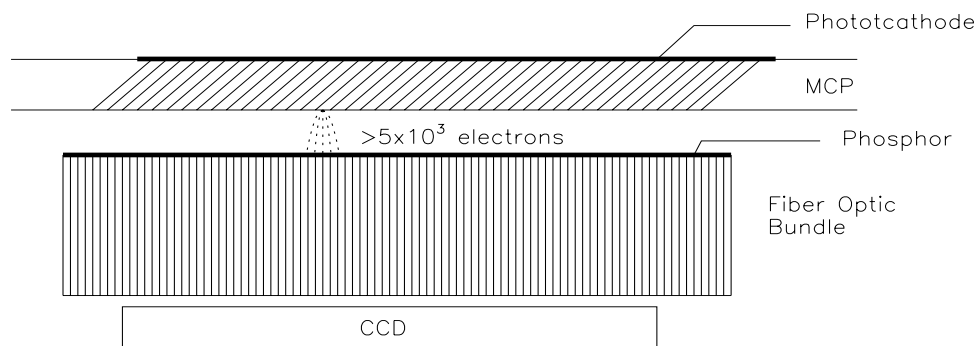

Fig. 3 schematic diagram of the MCP-Intensified CCD (ICCD).

Another type of UV detector in common use and sometimes confused with the ICCD is the electron-bombarded solid-state arrays such as the Digicons currently being used in the Faint Object Spectrograph (FOS) and the Goddard High-Resolution Spectrograph (GHRS) on the *Hubble* Space Telescope (Brandt *et al.* 1979). While the FOS and GHRS have excellent performance characteristics (e.g. Eck, Beaver, & Shannon 1985) and are operating outstandingly well in orbit (Troeltzsch *et al.* 1991, Harms & Fitch 1991), the electromagnetic focusing systems are bulky and heavy. This type of detector would be of little interest for future UV instruments were it not for the fact that an Electron-Bombarded CCD (EBCCD) with an opaque photocathode has achieved very high (> 70%) DQEs (Jenkins *et al.* 1988, Jenkins *et al.* 1989, Joseph & Jenkins 1991) and new-technology magnet designs will allow the weights to be reduced by factors of 3 (Lowrance, Joseph, Leupold, & Potenziani 1991, Joseph *et al.* 1995), making the weight of this device competitive with other UV and FUV detectors. The LDR for the EBCCD (schematically pictured in Figure 4) is also competitive with alternative devices. This device has been demonstrated to achieve signal-to-noise ratios in excess of 100 in two modes: 1) photon counting mode and analog mode in which multiple events are allowed to accumulate in a single pixel during a 1/15 second frame time.
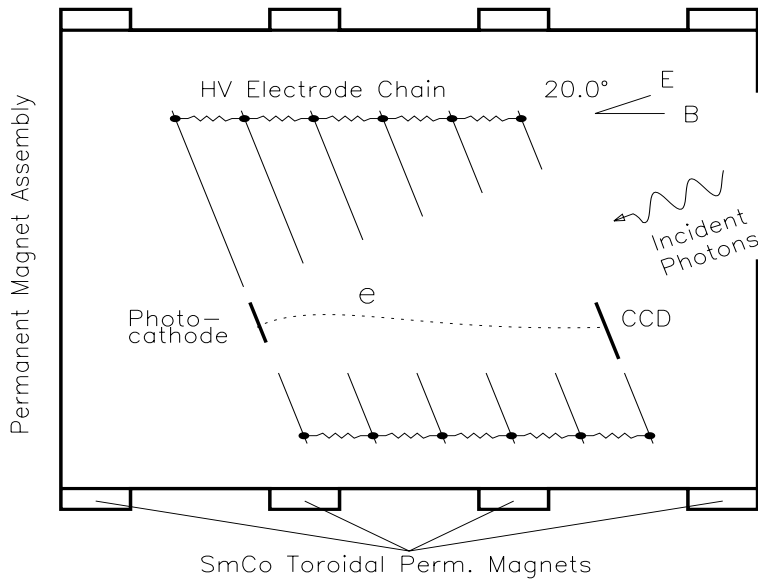
Fig. 4 schematic diagram of the Electron-Bombarded CCD (EBCCD),
which has flown successfully on sounding rockets and on the ORFEUS
orbital mission. The EBCCD offers the highest QE from a photocathode.

To summarize detector Quantum Efficiencies, Figure 5 shows the current status of QEs
and DQEs of common detectors. The top plot in Figure 5 shows the QEs that can be
obtained with various configurations of thinned, back-illuminated CCDs. The solid curve
shows a CCD with a typical antireflection coating, which has little QE response shortward
of 300 nm. Recently, SITe (formerly Tektronix) has developed a new antireflection (AR)
coating to be used by the Space Telescope Imaging Spectrograph (STIS) Program. This
AR coating, which has good near-UV response, is plotted as a solid curve with diamonds
in Figure 5 (Blouke *et al.* 1993). Future antireflection coatings, depicted as a dot-dash
line, may extend the range well into the UV. Likewise, delta doping of thinned chips has
the potential for significant UV enhancement of CCDs (Nikzad *et al.* 1994a,b). A lumogen
phosphor coating on a thinned chip has been demonstrated to have the QE shown by the
curve with solid dots. Unfortunately, when placed behind a Woods filter to make it insen-
sitive to optical wavelengths (solar blind), the QE drops to the level depicted by the bold
solid curve (WFPC2 Instr. Handbook, C. Burrows, editor 1994).

At the bottom of Figure 5 are the Solar-Blind Efficiencies or DQEs obtained by various
UV sensors. Once again the lumogen coated CCD plus Woods filter combination is plotted
with a bold-line curve. This DQE curve is for a pristine CCD/Woods combination before
contamination becomes a factor. (See §2.3 for further details.) All of the DQE curves
for the MCP detectors are actual demonstrated values (Joseph *et al.* 1994, Siegmund &
Gaines 1990) as is the FUV curve for the EBCCD (Jenkins *et al.* 1988). Plotted as dotted
lines in the bottom part of Figure 5 are the expected UV DQEs for two future EBCCDs.
These EBCCD curves incorporate all known losses such as that due to the entrance window.
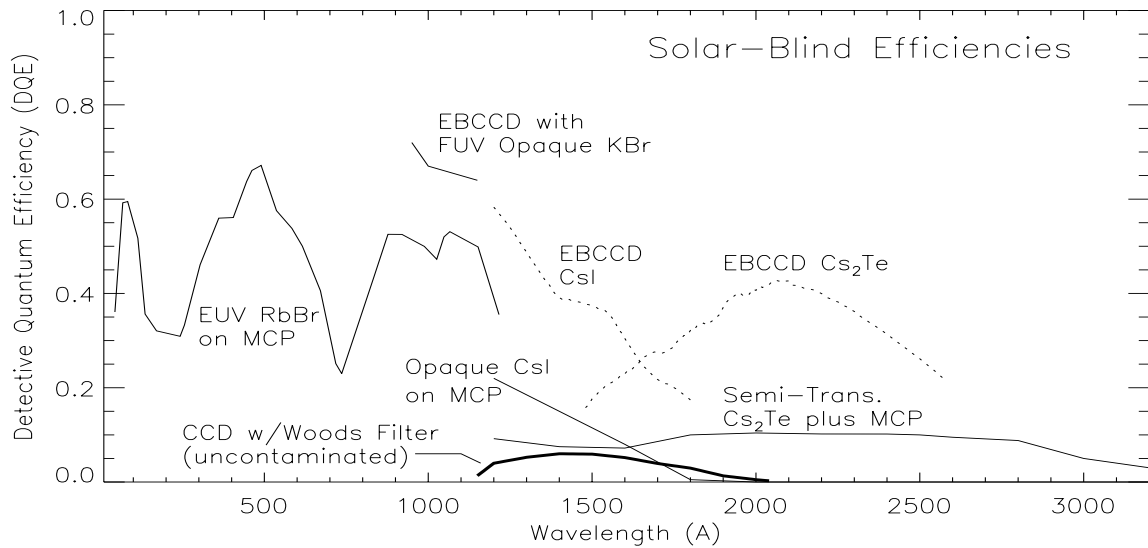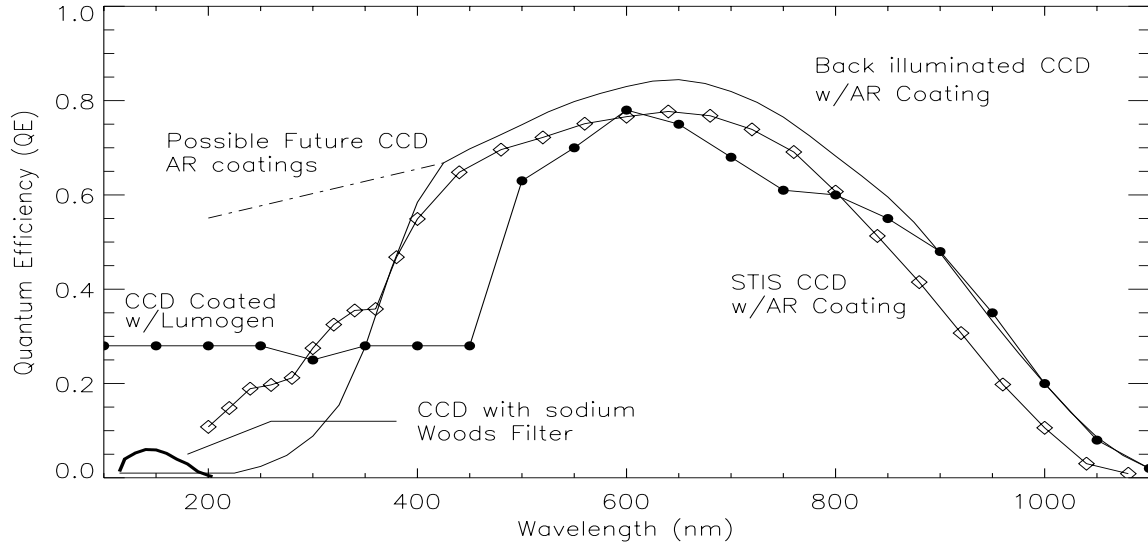
Fig. 5 showing QEs of various configurations of thinned back illuminated CCDs (top) and solar-blind UV DQEs of various detectors (bottom). The Woods filter transmission efficiencies are taken from the WFPC2 Instr. Handbook, C. Burrows, editor 1994 and the resulting DQEs combine these filter efficiencies with a 30% QE from the lumogen coated CCD. Note that very high (>80%) peak QE in the EUV range can be obtained with CCDs (Stern, Shing, & Blouke 1994), but solar-blind DQEs are lower than the MCP results for any reasonable assumption of filter efficiency. Also note that for many EUV applications, MCP-based detectors often incorporate a plastic or thin-film filter to block UV (not visible) lines which would lower the EUV DQEs below those plotted.

Figure 6 shows both Global- and Local- Dynamic Range envelopes for several important photoemissive devices. The distribution of light in the focal plane can significantly impact sensor performance. All envelopes in Figure 6 represent the 10% loss point (Joseph *et al.* 1994, Siegmund *et al.* 1992; Siegmund *et al.* 1994a, Dopita 1994). As an example, the distribution of light in the focal plane is shown for the medium resolution mode of STIS, denoted as "STIS: R = 2×10^4". In this medium-spectral resolution mode, the distribution of light on the detector from any hot star will fall somewhere along this dashed line. The particular form of parameterization in Figure 6 stems from the fact that separate physical processes set these limits for MCP-based detectors. The GDR for most MCP-based detectors is limited by the speed of the electronics which must process each photoevent sequentially. Coincidence losses occur when the photons arrive too rapidly. The LDR, on the other hand, is set by the recharge timescale of the MCP. When light is concentrated into a small region of the detector, rapid pulsing of the MCP can lead to incomplete recharging between pulses and a corresponding sag in gain (see Fraser *et al.* 1991; Fraser *et al.* 1993). Whenever the LDR is exceeded, the MCP becomes nonphotometric and introduces image distortions, especially for Z stack detectors (Siegmund & Stock 1991; Fraser *et al.* 1991; Fraser, Pain & Lees 1993).
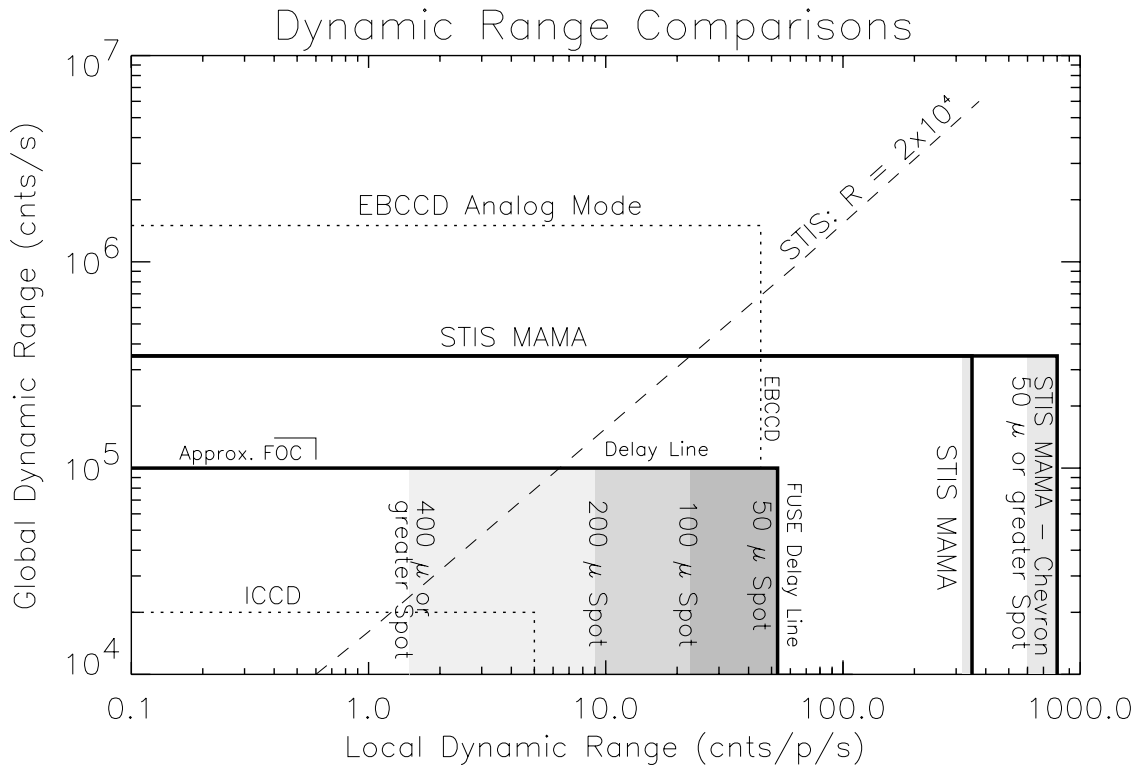

Fig. 6 showing dynamic range envelopes. All detectors have been normalized to a common size and electrical parameters (see text for details). The EBCCD Analog Mode allows multiple event pile up within a single frame time. (See Table 1 for references.)

To facilitate the comparison in Figure 6, all detector systems have been normalized to have a 1024 × 1024 format of square pixels each 25 μm on a side. The approximate envelope of the Faint Object Camera is shown in Figure 6 and is labeled "Approx. FOC". The electrical performances of all MCPs have been normalized to a resistance of 20 $M\Omega$ for a 40 mm plate. Different detector systems based on MCPs use various numbers of MCPs, sometimes with gaps between each. As a result, the LDRs for some of these devices are strongly dependent upon the scene being recorded. The shaded regions show the limits where simultaneous loss in resolution and photometry occur as a function of spot size. The LDR for the STIS MAMA in the Chevron Configuration, for example, is independent of spot size for spot diameters of 50 μm or larger. The Delay Line, however, has an LDR over 50 for a 50 μm spot but only an LDR of < 2 cnts/pixel/second for a 400 μm or greater diameter spot. The physics behind this phenomenon will be discussed in greater detail in the next subsection.

Table 1 provides an abridged overview of a few photoemissive detectors, showing relative performances in key parameters. For the MAMA and Delay Line, the top row of numbers for a given parameter constitutes the currently achieved values of the STIS MAMA in the chevron configuration and the Far Ultraviolet Spectroscopic Explorer (FUSE) Delay Line, respectively. Note: the FUSE Delay Line is really 3 butted Delay Lines and the values are for 1 of these 3 segments. A second value is given when other demonstrated detector configurations provide a significantly different capability.

One parameter not yet discussed, which is intangible but very important, is the level of maturity. For the present purposes a maturity of "Flight" indicates the detector has been used successfully on a sounding rocket or a short orbital mission. "Major Program" is used to indicate a serious engineering development has occurred as the result of a major flight mission.

Finally, lifetime is an important consideration. For CCDs cosmic ray hits not only limit the exposure times, these hits eventually degrade the charge transfer efficiency and increase the dark levels (e.g. Kimble *et al.* 1994). This degradation is more severe in high earth orbit than it is for low ones, but the effects of high earth orbit are still not well characterized. In preparation for AXAF-I, considerable study of the CCD radiation damage has already been performed by the Leicester group in the UK. NASA will soon be conducting an empirical assessment of the long-term CCD performance in high earth orbit. Similarly, the gain of an MCP diminishes as a function of the total charge extracted over time. This affect has been consequential in the past especially for sensor systems requiring very large amounts of charge per pulse, but for detectors with preconditioned plates, smaller amounts of diminished gains can be compensated with simple increases to the high voltage on the MCP (e.g. Siegmund *et al.* 1992; Joseph *et al.* 1994).

Table 1
Performance Comparisons for a Few Photoemissive Detectors

Parameter	MAMA	Delay Line	ICCD	EBCCD	Notes:
DQE	15-20%	15-20%	15-20%	50-60%	CsI at 121.6 nm
Vis. Reject.	$< 10^{-7}$	$< 10^{-6}$	$< 10^{-6}$	$< 10^{-6}$	CsI at 400 nm.
Max LDR	800 c/p/s	2-53 c/p/s	5 c/p/s	45 c/p/s	Delay Line scene dep.
Max GDR	3.5×10^5 c/s 9.0×10^5 c/s	1.0×10^5 c/s	2.0×10^4 c/s	1.5×10^6 c/s	at 10% Coinc. Loss
Array Size	1Kx1K 2Kx2K	13Kx3K	2Kx2K	1Kx1K	
Pixel Size	$25x25\mu^2$ $14x14\mu^2$	$20x32\mu^2$ $18x18\mu^2$	$7.5x7.5\mu^2$	$21x21\mu^2$	ICCD set by 1/2 of CCD pixel
Maturity	Flight & Major Prog.	Flight	Major Prog.	Flight	

References:

STIS MAMA:	Joseph *et al.*1994; Timothy 1991b
FUSE Delay Line:	Siegmund *et al.*1993; Siegmund *et al.*1994a
ICCD:	Dopita 1994
EBCCD:	Jenkins *et al.*1988; Joseph *et al.*1995

2.2   MCP Detectors Using An Anode Structure

Microchannel plate detectors using an anode structure can be divided into subtypes based on corresponding methods to encode the electrons clouds emerging from the back of the MCP. Some of these encoding schemes require stacks of MCPs with the spreading of charge to multiple channels in the second or third MCP to obtain sufficient gain. One of the simplest schemes to visualize is a single resistive anode where the location of the event is encoded via the amount of charge divided between amplifiers attached to the corners of the resistive anode (e.g. Barstow *et al.* 1985). There are other continuous encoding mechanisms for MCPs. These include 1) the Wedge and Strip anode (Martin *et al.* 1981), 2) the Spiral Anode (SPAN, Lapington *et al.* 1991, and 3) the Delay Line (Lampton *et al.* 1987, Siegmund *et al.* 1989; Friedman, Fleischman, & Martin 1992). Discrete anode structures, which use significantly more amplifiers and encode the location through direct detection, include: 1) the Multi-Anode Microchannel Array (MAMA, Timothy 1991b) and

2) the capacitive readout system of the Coded Anode Converter (CODACON,; McClintock *et al.* 1992). There are still other methods for determining the location of the charge cloud emerging from an MCP. An example is the crossed grid, which has been used on the Einstein and ROSAT missions as well as will be used for AXAF (Murray & Chappell 1988). (See Timothy [1991a] or Siegmund *et al.* [1992] for a detailed discussion of various types.)

One important MCP-based work horse that has been and continues to be used extensively is the Wedge and Strip. Its long history of successes and its relatively low expense to fabricate are prime reasons for the continued popularity of the Wedge and Strip even though other more advanced technologies are capable of providing much higher performance. The Extreme Ultraviolet Explorer (EUVE), for example, has a Wedge and Strip. This detector is known to exhibit significant fixed pattern noise (15% RMS pixel-to-pixel variations in sensitivity). Actually, these variations are due to stretched and compressed mapping regions of the detector. Dithering of the EUVE spacecraft is required to find weak absorption features in EUV continuum sources. While all continuous encoding devices suffer from mapping functions that drift slowly with operation, the Delay Line, a more advanced technology, has stretching and compressing maps that are an order of magnitude smaller than that of the Wedge and Strip. Consequently, its sensitivity variation are less. Likewise, current STIS MAMA detectors consistently achieve 3-4% RMS variations and the MAMA discrete-anode structure results in no spatial drifts. To facilitate a discussion of physical processes for state-of-the-art detectors, the present paper will focus on only two successful MCP detectors: the Delay Line and the MAMA, both of which have recently undergone or are expected to undergo further significant improvement in the near future.

There are several versions of Delay Lines being developed by various research groups. The basic principle of the Delay Line is straightforward. The charge cloud strikes an anode structure and two pulses begin propagating in opposite directions. The event position is encoded from the differences in the arrival times between these two charge pulses. Gas proportional counters have used Delay-Line readout systems for more than 25 years (e.g. Charpak *et al.* 1968). This encoding technique was first used with MCPs by the Rutherford group, which used an anode of parallel wires coupled to a wire-wound delay line (Bateman, Connoly, & Stephenson 1982; Duval, Bateman, & Peacock 1986). Other examples of wire-wound Delay Line systems include: Sobottka and Williams (1988), Williams and Sobottka (1989), and Friedman, Fleischman, and Martin (1992).

The Space Astrophysics Group at Berkeley has perhaps the most prodigious effort in Delay Line technology. Planar Delay Lines on a flat substrate that are suitable for space applications were introduced by Lampton, Siegmund, and Raffanti (1987) and subsequently in 2 dimensional format by Lampton, Siegmund, and Raffanti (1990). These Delay Lines are being developed for the Far Ultraviolet Spectroscopic Explorer (FUSE) to be launched in 1998. Other missions using Delay Lines supplied by this group include: ORFEUS (Hurwitz & Bowyer 1991), SOHO (Siegmund *et al.* 1994b), and various sounding rockets. The Berkeley group has also made important contributions to the development of opaque alkali-halide photocathodes deposited on the MCP for the EUV and FUV (Siegmund and Gaines 1990). Early Delay Lines of planar design provided less resolution along the Y- than in the X- axis.

New methods, however, may enable Y-axis event positions to be determined with about as much accuracy as the X-axis positions (Raffanti & Lampton 1993). Currently, X-axis resolution of 20 μm is possible with variations in resolution across the detector (Siegmund et al. 1994a). These Delay Lines overdigitize the event positions by about a factor of 10, providing the maximum retention of data resolution.

Unlike other continuous encoders, large format Delay Lines are readily possible since the position errors are small and only grow as the 1/3 power of the format size for a given gain (Lampton 1991). This capability makes the Delay Line well suited for very long formats such as those required by the Rowland circle spectrograph on FUSE. It should be noted that curved focal planes are frequently desirable, especially for large formats and the Berkeley group has extensive experience using MCPs that have been polished to create a curved front surface. An advantage enjoyed by the Delay Line is the tube fabrication tolerances which are not nearly as tight as those for the competing MAMA detector system. These tolerances make the Delay Line relatively less difficult to fabricate. The principal shortcoming of the Delay Line as with any detector using a Z stack is the strong scene-dependent LDR (Siegmund & Stack 1991). Gain sag is responsible for this LDR behavior and is well documented to be most pronounced for Z stack devices (Fraser et al. 1991; Fraser, Pain & Lees 1993). Figure 7 shows the physical process responsible for this limitation. The Delay Line requires at least $2 \times 10^7 e^-$ to achieve < 25 μm resolution (Williams & Sobottka 1989; Siegmund, Lampton, & Raffanti 1989). To achieve this level of gain, a Z stack such as that shown schematically in Figure 7 must have charge spreading between each MCP so that numerous MCP channels are activated in the final plate for each event. If a second photoevent occurs in a time interval comparable to- or shorter than- the recharge timescale and within a distance comparable to the final charge cloud, the second event will have significantly less gain because some of the channels in the third plate that would have participated in the event are still depleted of charge. Thus, the centroid of the second pulse will have a systematic error. In the example of Figure 7, the second photoevent will either not be detected or will be erroneously displaced to the right, if it is detected.

This scene-dependent LDR behavior is not a major issue for many FUV and especially EUV applications where the flux levels are generally significantly lower than typical observations in the 1200 to 2000 Å wavelength interval. Further, certain optical designs sometimes mitigate the LDR problem for the Delay Line. The Rowland Circle Spectrograph on FUSE, for example, should constrain the light perpendicular to the dispersion direction, preventing to some extent charge depletion contributions from locations perpendicular to the dispersion. For other formats such as those of the STIS instrument, for example, this scene-dependent LDR would have been an important disadvantage.
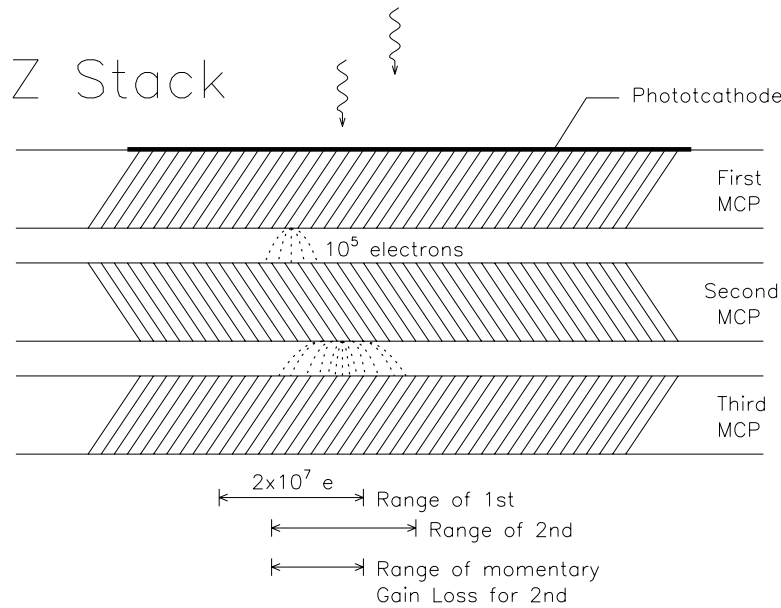
Z Stack

Phototcathode

First
MCP

10^5 electrons

Second
MCP

Third
MCP

2×10^7 e

Range of 1st

Range of 2nd

Range of momentary
Gain Loss for 2nd

Fig. 7 showing the physical process responsible for the strong scene-
dependent LDR for a Z Stack. All MCP detectors experience some loss of
photometry and image distortion near their LDR limit, but these
nonlinearities are significantly less for chevron stacks and even smaller for a
single MCP (see Fraser *et al.* 1991, Fraser *et al.* 1993).

For this and other performance reasons, the STIS project selected the Multi-Anode Mi-
crochannel Array (MAMA) detector. The STIS Instrument Team undertook a series of
MAMA tube builds with improvements having been implemented at each stage to provide
a sufficient heritage to insure fabrication success of the flight detectors. In concert with
other NASA and military programs as well as Ball Aerospace IR&D, STIS has advanced
a number of relevant technologies for the MAMAs (Joseph, Timothy, & Argabright 1991,
Danks *et al.* 1992., Corbett *et al.* 1992, Joseph *et al.* 1994). These include: 1) improve-
ments to the metallurgy of the anode arrays, 2) the design and fabrication of Application
Specific Integrated Circuits (ASICs) that have reduced the power and size of the electronics
as well as being more robust electronically, and 3) refining the methods of manufacture of
curved-channel MCPs.

In contrast to the success on the STIS Program with MAMAs, the NASA/ESA SOHO
Program ran into some difficulties and eventually abandoned the technology in favor of
Delay Lines. Also, the availability of sufficient numbers of good MCPs (both curved- and
straight- channel plates) continues to be problematic for the MAMAs, often impacting over-
all system performance. To help mitigate the shortage of suitable plates, the STIS MAMA
design has been altered somewhat to accommodate either curved-channel MCPs or small-

channel, tightly configured chevron stacks. Excellent performance has been demonstrated in both configurations (Joseph *et al.* 1994, see Table 1). The demonstrated capability of chevrons has additional benefits as well. For example, MCPs with curved surfaces are as readily available for MAMA detectors as they are for other formats. Further, smaller channel sizes can be obtained with chevron MCPs than with curved-channel MCPs increasing the resolution. The STIS MAMAs oversample the image by a factor of 4 to insure excellent spatial and spectral resolution.

Good tube yields have been realized in producing the STIS Engineering Model Units (EMUs) as well as with the flight MAMA detectors with some of the EMUs having performances suitable for flight. One of these EMU MAMAs has been operated for substantial periods of time after having undergone both shake and thermal environmental testing. An earlier demonstration tube has been used extensively for over a year to evaluate STIS gratings in the Goddard Diffraction Grating Evaluation Facility. The STIS MAMA Detectors have now matured to the point where half of the total test and evaluation effort is concerned with the characterization of subtle processes, a level of characterization needed to achieve data with a signal-to-noise ratio in excess of 100 (Joseph *et al.* 1994).

2.3   CCDs With Enhanced UV Sensitivity

There is considerable interest in adapting CCDs for UV applications (105 to 300 nm). CCDs are the detector of choice for Near-UV ($\lambda > 2000$ Å) and visible applications (Janesick *et al.* 1984; also see: *The Future of Space Imaging* 1993, R. Brown ed.; Astrotech 21, 1991 B. Wilson, ed.; Welsh 1992). NASA's desire, at least for the near UV, is manifested in the engineering efforts of the upcoming missions of the Stratospheric Aerosol and Gas Experiment (SAGE) and the Space Telescope Imaging Spectrograph (STIS) Projects. CCDs are desirable due to their reliability and compactness, qualities inherent in all solid state devices. In addition, CCD pixels form large potential wells so that images can be accumulated with a wide dynamic range in pixel intensities. CCDs are particularly well suited for high flux rates and high signal-to-noise applications. Often to achieve the latter one must first have the former.

Notwithstanding their enormous success at visible and near-UV wavelengths, the presently available CCD technology only achieves a solar-blind DQEs in the UV of 1-5% compared to 15-20% that routinely is obtained with MCP-based detectors. There are three technological hurdles to overcome before CCD DQEs will be competitive for general-purpose UV instruments. These are: 1) CCDs require some type of filter to block optical wavelengths. Many astronomical sources have their peak emission at optical wavelengths where the CCD has its maximum sensitivity and failure to exclude the optical flux sufficiently, introduces an enormous amount of contaminating noise into the UV observations. Although such filters do exist (e.g. Woods Filters - Trauger *et al.* 1994), the typical peak transmission rarely exceeds 20%. 2) CCDs must be kept cold to control the internal dark current. Condensibles form on any cold surface killing the UV transmission, even in a vacuum space environment.

To overcome this shortcoming, windows which can be kept warm can be introduced, but only for wavelengths longward of 1200 Å and only with a transmission efficiency of about 60-70% at the shortest wavelengths for common faceplate materials. 3) Even if the first two problems could be solved with 100% efficiency, current CCD technology is such that sensitivities for wavelengths below 200 nm are still no better than MCP-based detectors. Collectively, these problems are so acute shortward of 200 nm that no long-term general-purpose CCD has ever performed efficiently in orbit at ultraviolet wavelengths.

Most commercial off-the-shelf CCDs are thick, front-illuminated silicon chips, having limited visible QEs ($< 50\%$) due to the electronic gate structure deposited on the front. It is possible to make these sensitive to UV light by simply incorporating a phosphor in the CCD coating, which absorbs UV photons and re-radiates in the visible. UV Quantum Efficiencies of a few percent ($DQE < 1\%$ behind an optical blocking filter) have been achieved with these devices. WFPC2 on the HST has this basic unthinned architecture.

Thinning CCD chips and illuminating these from the backside dramatically improves their scientific usefulness at all wavelengths. Maximum QE at the optical wavelengths rise to 85% compared to 40% for thick chips. Similarly, phosphor coatings on thinned, backside illuminated chips have achieved higher QE at UV wavelengths than thick chips. QE's of 30% (DQE=6%) have been realized down to 1200 Å. Unfortunately, phosphors outgas inside evacuated tubes, resulting in a significant internal pressure and in the potential for changes in the coating's response. To prevent changes in the phosphor, WFPC2 used a hermetically sealed tube with 1.1 atmospheres of argon (C.J. Burrows, ed. 1994). Either with or without the argon, the tube configuration has a substantial pressure making it difficult to maintain a warm window to prevent condensing contaminates from forming on the window. These condensible contaminates are problematic even in the vacuum of space, lowering the UV response. Fortunately, thinned, back-illuminated CCDs also lend themselves more naturally to thin-film technologies capable of enhancing the UV sensitivity without outgassing problems (e.g. Blouke *et al.* 1993).

Similar to optical components, surface layers on CCDs play an important role in the overall efficiency of an instrument, especially at ultraviolet wavelengths. For example, the index of refraction of silicon is so high between 200 and 300 nm that 50-70% of the incident radiation is reflected from the surface without some type of Anti-Reflection (AR) coating (Robinson *et al.* 1991, Blouke *et al.* 1992). For wavelengths below 2000 Å, a classic AR coating does not work since the index of silicon falls below one in this region and varies rapidly. Virtually all of the UV radiation that does get transmitted into a silicon substrate, however, is absorbed within a distance of order 100Å.

For a CCD, this is still not the whole story since the work function of the native $Si - SiO_2$ surface forms a shallow potential well. Most of the charge induced by the UV radiation this close to the surface of the CCD remains trapped there until it is lost through recombination. Thus to be effective, a CCD thin film structure must not only have a suitable refractive index and extinction coefficient, but there must also be some mechanism that drives photogenerated charge away from the CCD surface and into the correct potential well formed

by the gate structure where it will be detected. This latter requirement may necessitate complex coatings such as an AR coating plus bias layer. A bias layer is a thin conducting layer used to establish an externally-generated voltage potential.

In other words, one has to get the UV photons into the silicon and then drive the photo-generated electrons away from the surface where these are created. In addressing the second part of the problem, several techniques have been developed to moderate or to reverse the undesirable small potential well that naturally forms at the surface. These include: 1) creating a repulsive electrostatic charge in the native oxide on the surface by soaking the CCD in nitric oxide gas (a strong oxidizer) or by exposing it to strong UV light in the wavelength range 200-250nm (Janesick *et al.* 1985), 2) applying a conducting bias gate on top of a thin insulating layer which is then held at a suitable potential (Janesick *et al.* 1987, Robinson *et al.* 1991); or 3) building in an electric field by a very shallow ion implant and laser annealing (Bosiers *et al.* 1986, Janesick *et al.* 1987, Stern *et al.* 1987, Tassin *et al.* 1989, Nikzad *et al.* 1994a,b).

In addressing the problem of getting the light into the silicon, Lick Observatory, Steward Observatory, and the former Tektronix group have had some successes in enhancing the UV sensitivity of CCDs simply by applying a single layer AR coating. Among the candidate materials studied thus far are: HfO_2 (Lesser 1987), and Si_3N_4 (Tektronix, Inc., reports to Ball Aerospace). Both of these materials are compatible with modern integrated circuit technology and have favorable optical properties. While the efforts at solving both parts of the problem represent a good start, most of these solutions require maintaining the CCD at cyrogenic temperature under vacuum. In addition, there are many other potential AR coating materials that have never been systematically explored, many of which hold significant promise especially at shorter wavelengths. The stability and repeatability of current thin-film AR Coatings also remain problematic.

2.4   Electron-Bombarded CCDs (EBCCDs)

Electron-Bombarded CCDs (EBCCDs) have been under development for a number of years at Princeton University, the Naval Research Laboratory, and other research centers (e.g. Picat *et al.* 1972, Lowrance *et al.* 1979, Lowrance & Joseph 1988, Opal and Carruthers 1989, Richard, Bergonzi, & Lemonier 1990, Lowrance *et al.* 1991). One EBCCD with an opaque photocathode has been used in the Interstellar Medium Absorption Profile Spectrometer (IMAPS) sounding rocket, which also successfully flew piggyback on the Orbiting and Retrievable Far and Extreme Ultraviolet Spectrometer (ORFEUS) Mission (Jenkins *et al.* 1989, Joseph & Jenkins 1991). Future missions incorporating an EBCCD include a reflight of ORFEUS/IMAPS in 1996 and an Air Force unmanned orbital mission, the Global Imaging Monitor of the Ionosphere (GIMI).

The IMAPS detector, which was shown schematically in Figure 4, is described extensively in Jenkins *et al.* (1988). Basically, it consists of a photocathode surface, an accelerating electrostatic field of several thousand volts to accelerate the photoelectrons, and a thinned, backside illuminated CCD. A photoelectron striking the CCD produces approxi-

mately one secondary electron for every 3.6 eV of incident energy (Reinheimer 1990). In practice, photoelectrons in the IMAPS detector having 18.5 KeV pass through a 3 KeV dead layer, producing approximately 3,000 electron-hole pairs. Each photoevent is localized in a width having an exponential (rather than Gaussian) spread with a scale length of 4-6 μm in the CCD. The entire CCD image is read at a rate of 15 hertz and individual photoevents identified. The CCD is operated warm with a dark level of 1500-7500 electrons and a readout noise of 70 electrons. The EBCCD with an opaque photocathode on a smooth surface achieves the highest quantum efficiency currently available (DQE > 70%; Jenkins et al. 1988, Jenkins et al. 1989, see Figure 5). A magnetic field is required to shift the photoelectrons out of the optical path and towards the CCD as shown in Figure 4.

The CCD used by IMAPS is a thinned, back illuminated RCA CCD with 320×512 pixels that are 30 μm on a side. The CCD is divided into two registers of 320×256 each and is operated in a frame-transfer mode. The first register is open and accumulates the next 1/15 second integration, while the covered register serves as an image buffer of the previously integrated frame. Each frame is processed in real time and an external memory updated. At the end of each read, the first register is rapidly transferred to the other to prevent image smearing and the next integration/read begins.

The Local- and Global- Dynamic Range envelopes are shown in Figure 6. The IMAPS EBCCD is simultaneously capable of photon-counting detection and analogue mode operation for high flux levels where event crowding occurs for the 1/15 second frame rates. In the latter mode, the signal from multiple photoevents is converted analog-to-digitally and the signal added to the existing signal in an integrating memory. If ions enter the detector, or are created therein, these will be accelerated toward the photocathode, creating 10 to 20 free electrons. These electrons will be electromagnetically focused onto the CCD within about a pixel size and are easily discriminated out.

As with all detectors in this classification type, the EBCCD has some S and pin-cushion distortions. For the IMAPS detector these were small ($\lesssim$0.5% Jenkins et al. 1988). Image deflection is also possible as a result of different orientations with respect to the earth's magnetic field. The detector produces external magnetic flux usually requiring a compensating magnet elsewhere on the spacecraft to prevent unwanted torques on the attitude control system. Although the IMAPS device uses a bulky magnet design that is heavy and leaks substantial amounts of magnetic flux, the high DQE is effective with small telescope apertures, making the overall instrument light. No sealed tube design for an EBCCD has been developed for operation longward of 1216 Å. Nevertheless, new tube designs, which will be discussed in §3, offer significant improvements in a number of these present limitations, especially in reducing the weight.

3 Future UV Detector Technologies

3.1 Near-Term Future Technologies

Research groups in Europe, many funded through the European Space Agency (ESA), are developing CCDs for various space applications. The Leicester group has performed extensive studies on in-orbit proton damage to CCDs (Holland *et al.* 1990). Other UV/EUV CCD efforts are being made by the Padua group led by Tondello. (See contributions to the ESA Symposium on Photon Detectors for Space Instrumentation 1992 [ESA SP-356]).

Similarly, several research groups in the US are actively pursuing CCD technologies to enhance the UV sensitivities of these devices. Stewart Observatory has been experimenting with thinning Loral chips and applying Anti-Reflection (AR) coatings (Lesser 1993). JPL is attempting to perfect two versions of phosphor coatings of lumogen (J. Janesick, PI). The first version is a low-cost, low-risk unthinned chip, while the other is a higher risk/cost thinned device offering high performance. A key element of this JPL effort are some design changes to the CCD architecture that may significantly reduce the CCD backgrounds. (Figure 1 suggests this should be feasible since one is not up against a thermodynamical limitation.) If this later portion of the effort is successful, the CCD could operate at a warmer temperature which would significantly lessen the condensation problems. A second JPL effort is using molecular beam epitaxial (MBE) methods for ion implantation of thinned CCDs to eliminate the unwanted potential well near the surface (P. Grunthaner, PI). Surface damage has been observed in the past with various methods of ion implantation. This damage tends to increase the mobility of the free charge (i.e. reducing the recombination time), which in turn, effectively reduces the ultraviolet QE since more of the charge is lost before it can be collected at the gates. The JPL ion implantation effort known as "delta-doping" has produced promising results for a highly-stable surface structure (Hoenk & Grunthaner 1992, Nikzad *et al.* 1994a,b).

In addition to studies being conducted for various flight programs, the Space Astronomy Group (SAG) at Berkeley has two NASA funded programs to continue developing Delay Line technologies (O. Siegmund, PI; M. Lampton, PI). The primary goals are to increase resolution, increase format size, and increase speed. For soft X-ray and EUV sensors, the Leicester group has been developing very low noise (radioisotope free) MCPs (Fraser, Pearson, & Lees 1987; Fraser 1989). While this effort undertaken for the AXAF-I High Resolution Camera, all MCP detectors used in the UV would also benefit from even lower backgrounds.

Electron Bombarded CCDs using new magnet assemblies designed by the US Army Electronics Technology and Devices Laboratory are being developed by Princeton Scientific Instruments (J. Lowrance, PI). Field uniformity and flux confinement are attained with minimal structural mass through the principle of permanent magnet cladding. The basic principle is as follows. Supply magnets that generate the internal field are cladded with additional magnets of appropriate size and orientation to create an equipotential at the outer surface. Accordingly, flux lines cannot extend between surfaces of the same magnetic potential if the surfaces are separated by media of finite permeability. (See Clarke & Leupold [1986] and Potenziani *et al.* [1987] for a discussion of this principle.) As noted the

EBCCD with an opaque photocathode offers very high quantum efficiency. Now the device will soon be fabricated with a 3-fold reduction in weight (Lowrance, *et al.* 1991).

There is on-going work at University College, London as well as Imperial College to improve large-format, intensified CCD detectors. This effort, headed by J. Fordham, is developing the Microchannel plate Intensified CCD or MIC Detector for the X-ray Multi-Mirror Mission (XMM), an ESA 'Horizon 2000' space observatory to be launched in 1999 (Fordham *et al.* 1991; Kawakami *et al.* 1994). In the United States, Charge Injection Devices (CIDs) are actively being developed (Carbone *et al.*, 1993). CIDs are similar to CCDs but each pixel contains a MOS capacitor so the CID can perform nondestructive reads on an arbitrary set of pixels. The architecture of the CID has many electrodes connected to each column line and row line resulting in a high line capacitance and corresponding low voltage change per unit charge. Consequently, CIDs traditionally have had a readout noise that is 10-20 times higher than CCDs, which has limited the use of simple CIDs for astronomy. However, when optically coupled to the output of an MCP-based intensifier analogous to an ICCD, the addressable readout capability of the CID can be used to enhance the LDR of the system in selected regions as demanded by the brightness distribution of the image or spectrum. Such "ICIDs" are currently being developed in a program at the Goddard Space Flight Center (R. Kimble, PI).

Another item of note for short-term developments is the self-calibrating spectrometers for EUV studies of the solar-upper atmosphere. Instrumental response especially in the EUV can change dramatically. The ATON (Egyptian Sun God) Mission will carry auto-calibrating EUV (2 to 140 nm) spectrometers which use gas chambers to establish an absolute calibration reference (Schmidtke 1992; Schmidtke *et al.* 1994). There is a clear and pressing need to measure with high precision and accuracy the solar EUV irradiance at wavelengths shortward of 1200Å since this is the dominant energy input to the region (see Lean 1991).

3.2 Long-Range Technologies

Looking much further into the future, there are several promising technologies that while these are still in their infancy, could ultimately make major advances to UV/FUV/EUV image sensors. For example, JPL has an on-going program to develop Active Pixel Sensors (APS, E.R. Fossum, PI). An APS detector is similar to a CCD but has at least one active transistor within the pixel unit cell, eliminating the need for nearly perfect charge transfer (Fossum 1993). The effectiveness of the charge transfer for a large-format solid state imager say with 8192×8192 pixels, for example, has only a fractional output of 0.849 after 8192 register shifts for a Charge Transfer Efficiency of 0.99999. The APS may overcome several difficulties associated with CCDs caused by the need for perfect charge transfer. These include: 1) difficulty of manufacture in large array sizes, 2) difficulty of interfacing with on-chip electronics, 3) difficulty of using at high frame rates, and 4) difficulty of manufacture in non-silicon materials that may be better for UV applications (Fossum 1993). APS technology is also just emerging in the most advanced imager laboratories in Japan for use in still cameras and high- definition television.

Another technology under development that holds real promise for UV image sensors are photoconductive detectors based on diamond (Marchywaka et $al.$ 1994) or on GaAlN substrates (Ulmer, Razeghi, & Bigan 1995). The band gap between valence and conduction bands is much larger for these substrates than for silicon, making these devices inherently superior for UV applications. Single pixel devices have been fabricated and tested at the Naval Research Laboratory (Marchywaka et $al.$ 1994).

The University of Wisconsin has a program to develop Advanced-Technology MCPs (AT-MCPs, C. Joseph, PI) which is piggybacking off a much larger, multimillion dollar effort being conducted by Galileo Electro-Optics Corp. and the National Institute of Standards and Technology. An AT-MCP, pictured in Figure 8, represents a radical departure in the use of materials and in the fabrication methods of MCPs. Rather than the glassy technologies developed in the 1960's, AT-MCPs use techniques and very pure materials developed by the semiconductor industry (Horton, Tasker, and Fijol 1990; Tasker, Horton, and Fijol 1990). These new process techniques remove many restrictions associated with traditional methods, enabling AT-MCPs to be inherently superior to conventional MCPs in seven different performance parameters.

Fig. 8 showing AT-MCP channels etched into silicon. Image taken from Horton, Tasker, and Fijol (1990).

One of the most important performance improvements offered by AT-MCPs is 1-2 orders of magnitude increase in LDR, making MCP detectors competitive with large-pixel CCDs. Channel activation for electron multiplication in an AT-MCP is achieved by thin-film deposition or growth along the channel walls, another technique of the semiconductor industry. These new channels are likely to have recharge times approaching 100 μs at gains of $10^5 - 10^6$ electrons, supporting a count rate of 10^3 to 10^4 per channel per second, more than a factor of 20 better than current MCPs. Greater gain stability and MCP lifetime is

realized by use of electron emissive films which are chemically inert, hermetic, and resistant to electron radiolytic damage.

In addition to the advantages introduced by the use of advanced materials, the fact that the array of channels in an AT-MCP has long-range order adds significant engineering flexibility to overcome several shortcomings. For example, AT-MCPs will significantly reduce the image distortions currently introduced by conventional MCPs (Hassler, Rottman, & Lawrence, 1990). AT-MCPs can be fabricated in formats that are larger than is mechanically sound for conventional MCPs. Furthermore, AT-MCPs are more suitable for mosaics.

Finally, Lawrence Livermore is conducting studies on sensors made out of low-temperature superconducting materials (S. Labov, PI). This new class of detector offers the possibility of 2-dimensional sensor with energy resolution (Drukier *et al.* 1991). Arrays of 256×256 superconducting grains with stable properties may be possible based on preliminary work. The long-ranged goal is to produce $2K\times2K$ arrays with 1% energy resolution, UV DQEs of at least 80%, and temporal resolutions of a few nanoseconds. Such a device would complement deep-depletion CCDs that are being developed to provide simultaneous position and energy information for use at soft x-ray wavelengths (Janesick *et al.* 1988; Garmire *et al.* 1988; Lumb & Holland 1988). Another approach, currently being pursued for X rays but that can be extended to the UV and visible, is that of superconducting tunnel junctions (e.g. Perryman, Foden, & Peacock 1993)

3.3   Summary and External Factors

The present review has shown that no detector system is well suited for all applications. This statement will likely remain valid for many years to come. For instance, Electron-Bombarded CCDs may offer theoretically the highest Detective Quantum Efficiency from a photocathode detector, but the need for high voltage will eventually inhibit further progress to scale down the size of the device. In contrast, AT-MCPs will permit substantial reductions in detector size and weight compared to existing detectors, but even with the enhanced DQE over conventional MCPs, it will not match the DQE of the EBCCD. Thus, for large instruments in low-earth orbits, the EBCCD might be the detector of choice, while a very light-weight detector based on the AT-MCP might be preferred for a spacecraft placed far from earth.

In some wavelength intervals, especially at shorter EUV wavelengths, CCDs will have greater QE than any MCP-based or other photoemissive device. In those few cases where solar blindness is unimportant, the CCD may be the detector of choice. The CCD may be the detector of choice for applications where very large flux rates are obtained in a few second integrations. In high earth orbit, however, radiation damage may preclude the use of silicon CCDs for any extended missions. There are many more performance trade offs that could be made to feature one detector system or another. This section only provides a couple of examples to demonstrate the point.

While emerging detector technologies have the potential to revolutionize many fields of astronomical study, future developments will depend more than ever on external pressures such as economic factors. NASA has traditionally used the resources of major flight programs to mature various technologies. Technological advances usually require a financial investment that is an order of magnitude higher than the recurring costs of a given detector. Today, efforts to make all flight programs (both small and large) leaner and quicker than past ventures may adversely impact technological progress. Furthermore, the complementary photoconductive and photoemissive technologies have relied heavily on commercial solid-state interests and on military night-vision interests, both of which have recently been in significant turmoil and subject to the vagaries of decision makers. Unless there is a source of significant and consistent financial support, the availability of high-quality large-format CCDs and MCPs simply cannot be guaranteed, let alone advanced.

The picture in Europe is somewhat better. Currently, the European Space Agency (ESA) has a Technology Research Program, which contains a significant number of budget lines specifically for the development of photon-counting UV/EUV/X-ray technologies (Fraser - private comm.). These include: 1) large-area, small-channel MCPs, perhaps with development efforts similar to the AT-MCP noted above, 2) small-pixel CCDs, and 3) back-illuminated CCDs. These research efforts are adequately funded and are typically 3-year in duration.

4 Acknowledgements

5 References

1. Barstow, M.A., Fraser, G.W., & Milward, S.R. 1985, SPIE *X-ray Instrumentation in Astronomy,* 697, p. 352.

2. Bateman, J.E., Connoly, J.F., & Stephenson, R. 1982, Rutherford Appleton Laboratory, RL-82-080.

3. Blouke, M.M., Nelson, M.D., Serra, M., Knoesen, A., Higgins, B.G., Delamere, W.A., Womack, G., Flores, J.S., Duncan, M., and Reed, R. 1992 SPIE, vol 1656.

4. Bosiers, J.T., Saks, N.S., McCarthy, D., Peckerar, M.C., and Michels, D.J. 1986, SPIE, 687, 126.

5. Brandt, J.C. & the GHRS Science Team 1979, SPIE, *Instrumentation in Astronomy III,* 172, p. 254.

6. Brown, R.A., Editor 1993, "The Future of Space Imaging", Report of a Community-Based Study of an Advanced Camera for the Hubble Space Telescope.

7. Burrows, C., editor 1994, Wide Field and Planetary Camera 2 Instrument Handbook, STScI publication (May 1994).

8. Carbone, J., Zarnowski, J.J., Arnold, F.S., & Hutton, J. 1993, *Proc. SPIE, Charge-Coupled Devices and Solid State Optical Sensors III,* 1900, 170.

9. Carruthers, G.R. 1993, Chapter 15 entitled: "Ultraviolet And X-Ray Detectors", in *Electro-Optics Handbook,*R.W. Waynant & M.N. Ediger, editors, McGraw-Hill Inc.

10. Charpak, G., Bouclier, R., Bressani, T., Favier, J., & Zupancic, C. 1968, *Nucl. Instrum. & Meth.,* 65, 217.

11. Clarke, J.P., & Leupold, H.A., 1986, *IEEE Transactions on Magnetics,* 22, 5.

12. Corbett, M.B., Feller, W.B., Laprade, R. Cochran, Bybee, R., Danks, A., Joseph, C. 1992, SPIE

13. Danks, A.C., Joseph, C., Bybee, R., Argabright, V., Abraham, J., Kimble, R., & Woodgate, B. 1992, *Proc. of an ESA Symp. on Photon Detectors for Space Instrumentation,* held at ESA/ESTEC, Noordwijk, The Netherlands, 10-12 November 1992 (ESA SP-356. Dec. 1992).

14. Davidsen, A.F. *et al.* 1992, ApJ 392, 264.

15. Dopita, M.A. 1994, "The Starlab/Endeavor Photon Counting Array Detector: Capabilities for use in the UV detector of Advanced Camera". A report to the JPL Advanced Camera Science Advisory Committee.

16. Drukier, A.K. *et al.* 1991, *Proc. 4th Workshop on Low Temp. Detectors,* Oxford 1991.

17. Duval, B.P., Bateman, J.E., & Peacock, N.J. 1986, *Rev. Sci. Instrum.,* 57(8), 2156.

26

18. Eccles, M.J., Sim, M.E., & Tritton, K.P. 1983, *Low Light Level Detectors in Astronomy,* Cambridge University Press.

19. Eck, H.J., Beaver, E.A., & Shannon, J.L. 1985, *Advances in Electronics and Electron Physics,* 64A, p. 141.

20. Fordham, J.L.A., Bone, D.A., Oldfield, M.K., & Bellis, J.G. 1991, in Photoelectronic Image Devices, ed. B.L. Morgan, Institute of Physics Conference Series No. 121, pg 105.

21. Fossum, E.R. 1993, SPIE *Charge-Coupled Devices and Solid State Optical Sensors III, M.M. Blouke, editor* 1900, 1.

22. Fraser, G.W. 1989, SPIE, 1140, 50.

23. Fraser, G.W. 1989, *Detectors for X-Ray Astronomy,* Cambridge University Press, New York.

24. Fraser, G.W., Pearson, J.F., & Lees, J.E. *Nucl. Instr. Meth.*, A254, 447.

25. Fraser, G.W., Barstow, M.A., and Pearson, J.F. 1988, *Nucl. Instr. Meth.*, A273, 667.

26. Fraser, G.W., Pain, M.T., & Lees, J.E. 1993, *Nucl. Instr. Meth. in Physics Research*, A327, 328.

27. Fraser, G.W., Pain, M.T., Lees, J.E., & Pearson, J.F. 1991, *Nucl. Instr. Meth. in Physics Research*, A306, 247.

28. Friedman, P.G., Fleischman, J., & Martin, C. 1992, *in Proc. of 10th Intl. Coll. on UV and X-ray spectroscopy of Astrophysical Lab Plasmas, Berkeley, California.*

29. Garmire, G.P., Nousek, J., Burrows, D., Ricker, G., Bauntz, M., Doty, J., Collins, S., Janesick, J., Mountain, R.W., & Burke, B.E. 1988, SPIE *X-ray Instrumentation in Astronomy II,* 982, 123.

30. Gonsiorowski, T. 1986, *in Proc. SPIE Instrumentation in Astronomy IV* 627, 626.

31. Harms, R.J. & Fitch, J.E. 1991, SPIE *Space Astronomical Telescopes* in Astronomy, 1494, p. 49.

32. Hassler, D.M., Rottman, G.J., & Lawrence, G.M. 1990, *Proc. of SPIE*, 1344.

33. Hoenk, M.E. & Grunthaner, P.J. 1992, *Appl.Phys.Lett.*, 61, 1084.

34. Holland, A.D. *et al.*, 1990, *in Proc. SPIE*, 1344, 378.

35. Horton, J.R., Tasker, G.W., and Fijol, J.J. 1990, *SPIE*, **1306,** 169.

36. Hurwitz, M., & Bowyer, S. 1991, *in Extreme Ultraviolet Astronomy,* R. Malina and S. Bowyer, eds. (New York: Pergamon Press).

37. Janesick, J.R., Campbell, D., Elliott, T., and Daud, T. 1987, Optical Engineering., 26(9), 852.

38. Janesick, J.E., Elliott, T., Bredthauer, R., Chandler, C., & Burke B. 1988, SPIE *X-ray Instrumentation in Astronomy II*, 982, 70.

39. Janesick, J., Elliott, T., Collins, S., Marsh, H., Blouke, M. Freeman, J. 1984, SPIE 501, 1.

40. Janesick, J.R., Elliott, S.T., Daud, T., McCarthy, J., and Blouke, M.M. 1985, SPIE, 570, 46.

41. Jenkins, E.B., Joseph, C.L., Long, D., Zucchino, P.M., Carruthers, G.R., Bottema, M., & Delamere, W.A. 1988, SPIE *Ultraviolet Technology II*, 932, p. 213.

42. Jenkins, E.B., Lees, J.A., van Dishoeck, E.F., & Wilcots, E.M. 1989, ApJ, 343, 785.

43. Joseph, C.L. Argabright, V., Bybee, R., Danks, A., & Woodgate, B. 1994, *Proc. SPIE Ultraviolet Technology V*, 2282, 116.

44. Joseph, C.L. & Jenkins, E.B. 1991, ApJ. 368, 201.

45. Joseph, C.L., Lowrance, J.H., Leupold, H., & Potenziani, E. 1995, in prep.

46. Joseph, C.L., Timothy, J.G., and Argabright, V 1991, *B.A.A.S.,* **23**, 906.

47. Kawakami, H., Bone, D., Fordham, J., & Michel, R. 1994, *Nucl. Instr.Meth.*, A348, 707.

48. Kimble, R., Brown, L., Fowler, W., & Woodgate, B., 1994, *Proc. SPIE Ultraviolet Technology V,* 2282, 169.

49. Lampton, M.L. 1991, invited review for *Extreme Ultraviolet Astronomy,* R.F. Malina and S. Bowyer, eds., (New York: Pergamon Press).

50. Lampton, M., Siegmund, O.H.W., & Raffanti, R. 1987, *Rev. Sci. Instrum.*, vol. 58, no 12, p. 2298.

51. Lampton, M., Siegmund, O.H.W., & Raffanti, R. 1990, *IEEE Trans. Nucl. Sci.,* 37, 1548.

52. Lapington, J.S., Breeveld, A.A., Edgar, M.L., & Trow, M.W. 1991, *Nuclear Instr. and Methods in Physics Research,* A310, 299.

53. Lean, J. 1991, *Rev. Geophys.,* vol. 29, No 4, p. 505.

54. Lesser, M.P. 1993, SPIE *Charge-Coupled Devices and Solid State Optical Sensors III, M.M. Blouke, editor* 1900, 219.

55. Lesser, M. 1987, Optical Engineering, 26, 911.

56. Lowrance, J.L., & Joseph, C.L. 1988, *in Adv. in Electronics and Electron Physics,* 74, p. 465.

57. Lowrance, J.L., Joseph, C.L., Leupold, H., & Potenziani, E. 1991, *in Photoelectronic Image Devices 1991,* ed. B.L. Morgan, Institute of Physics Conference Series No. 121,

58. Lowrance, J.L., Zucchino, P., Renda, G. & Long, D.C. 1979 *in Adv. E.E.P.,* vol. 52, p. 441.

59. Lumb, D.H. & Holland, A.D. 1988, SPIE *X-ray Instrumentation in Astronomy II,* 982, 116.

60. Malina, R.F., Bowyer, S., Lampton, M., Finley, D., Paresce, F., Penegor, G., and Heetderks, H. 1982, *Opt. Eng.* , **21**, 764.

61. Marchywaka, M., Binari, S.C., Pehrsson, P.E., & Moses, D. 1994, SPIE *Ultraviolet Technology V* 2282, 20.

62. Martin, C., Jelinsky, P., Lampton, M., Malina, R.F., & Anger, H.O., 1981, *Review of Scientific Instruments,* p1067.

63. McClintock, W.E., Lawrence, G.M., Kohnert, R.A., & Esposito, L.W. 1992, *Proc. SPIE,* 1745.

64. Murray, S.S., & Chappell, J.H. 1988, SPIE X-ray Instrumentation in Astronomy II, 982, p. 48.

65. Nikzad, S., Hoenk, M.E., Grunthaner, P.J., Terhune, R.W., & Grunthaner, F.J. 1994a, SPIE, 2217.

66. Nikzad, S., Hoenk, M.E., Grunthaner, P.J., Terhune, R.W., & Grunthaner, F.J. 1994b, SPIE, 2278.

67. Opal, C.B., & Carruthers, G.R. 1989, *in Proc. SPIE, Ultraviolet Technology III,* vol 1158, p. 96.

68. Papalios, C. & Mertz, L. 1982, in Proc. SPIE *Instrumentation in Astronomy IV* 331, p. 360.

69. Perryman, M.A.C., C L Foden, C.L., & Peacock, A. 1993 *Nucl. Instruments & Methods,* A325, 319.

70. Picat, J.P., Combes, M., Felenbok, P., & Fort, B. 1972, *in Adv. E.E.P.,* vol 33A, p. 557.

71. Potenziani, E., Clarke, J.P., & Leupold, H.A. 1987, *Appl. Physics,* 61, 8.

72. Raffanti, R. & Lampton, M. 1993, *Rev.Sci.Instrum.,* 64(6), 1506.

73. Ramsey, B.D., Austin, R.A., & Decher, R. 1994, *Space Science Reviews,* 69, 139.

74. Reinheimer, A.L. 1993, SPIE, vol. 1900, p. 69.

75. Richard, J.C., Bergonzi, L., & Lemonier, M. 1990, SPIE Vol 1338, p. 241.

76. Robinson, L., Brown, W., Gilmore, K., Stover, R., and Wei, M. 1991, SPIE, 1447, 214.

77. Roberts, E.H., Tuohy, I.R., & Dopita, M.A. 1988, *Advances in Electronics and Electron Physics,* 74, p. 297.

78. Schmidtke, G. 1992, *Proc. SPIE* Vol 1764, p. 72.

79. Schmidtke *et al.* 1994, *Proc. SPIE Ultraviolet Technology V,* 2282, 145.

80. Siegmund, O.H.W. 1991, Report for FUSE, August 1991.

81. Siegmund, O.H.W., Chakrabarti, S., Cotton, D.M., and Lampton, M. 1989, *IEEE Trans. Nucl. Sci.,* NS-36.

82. Siegmund, O.H.W., & Gaines, G.A. 1990, SPIE, *EUV, X-ray and Gamma-ray Instrumentation in Astronomy,* 1344, p. 217.

83. Siegmund, O.H.W., Gummin, M.A., Stock, J., & Marsh, D. 1992, *in Proc. of an ESA Symp. on Photon Detectors for Space Instrumentation,* held at ESA/ESTEC, Noordwijk, The Netherlands, 10-12 November 1992. (ESA SP-356, Dec. 1992).

84. Siegmund, O.H.W., Gummin, M.A., Stock, J., Marsh, D., Sasseen, T., Raffanti, R., & Hull, J. 1994a, Preprint entitled: "Delay line microchannel plate detectors for the Far Ultraviolet Spectroscopic Explorer Satellite."

85. Siegmund, O.H.W., Lampton, M.L., & Raffanti, R. 1989, *Proc. SPIE,* 1159, 476.

86. Siegmund, O.H.W. *et al.* 1994b, SPIE, 2280, 89.

87. Sobottka, S., Williams, M.B. 1988, *IEEE Trans. Nuc. Sci.,* NS-35(1), 348.

88. Stern, R.A., Catura, R.C., Kimble, R., Davidson, R., Winzenread, M., Blouke, M.M., Hayes, R., Walton, D.M., and Culhane, J.L. 1987, Optical Engineering, 26(9), 875.

89. Stern, R.A., Shing, & Blouke, M. 1994, *Applied Optics,* 33, 2521.

90. Tasker, G.W., Horton, J.R., and Fijol, J.J. 1990, MRS Symposium Proceedings, 192, 459.

91. Tassin, C., Thenoz, Y., Lemaitre, R., and Chabbal, J. 1989, SPIE, vol. 1140.

92. Timothy, J. G. 1983, *Pub.Astron.Soc.Pacific,* 95, 810-834, (invited review paper).

93. Timothy, J. G. 1985, IEEE Transactions on Nuclear Science, NS-32, 427-432.

94. Timothy, J. G. 1991a, invited review in Photoelectronic Image Devices 1991, ed. B.L. Morgan, Institute of Physics Conference Series No. 121, p.

95. Timothy, J. G. 1991b, in Photoelectronic Image Devices 1991, ed. B.L. Morgan, Institute of Physics Conference Series No. 121, p. 85.

96. Timothy, J. G., and Madden, R. P. 1983 invited review chapter in Handbook on Synchrotron Radiation, Vol. I, E. E. Koch, ed., North-Holland Publishing Company, 315-366,

97. Trauger, J.T. *et al.* 1994, ApJL, 435, L3.

98. Troeltzsch, J.R., Ebbetts, D.C., Garner, H.W., Tuffi, A., Breyer, R. Kinsey, J., Peck, C. Lindler, D., & Feggans, J. 1991, SPIE, *Space Astronomy Telescopes and Instruments,* 1494, p. 9.

99. Ulmer, M.P., Razeghi, M., & Bigan, E. 1995, SPIE, *presented at Photonics West, Spring 1995.*

100. Welsh, B.Y. 1992, in Proceedings of an ESA Symp. on Photon Detectors for Space Instrumentation, held at ESA/ESTEC, Noordwijk, The Netherlands, 10-12 November 1992. (ESA SP-356, Dec. 1992).

101. Williams, M.B., & Sobottka, S. 1989, *IEEE Trans. Nuc. Sci.,* NS-36(1), 227.

102. Williams, J.T. & Weistrop, D. 1983, SPIE *Instrumentation in Astronomy V,* 445, p. 204.

103. Wilson, B., editor 1991, "Workshop Proceedings: Sensor systems for Space Astrophysics in the 21st Century", Astrotech 21 Series III, JPL Publication 91-24, Vol 3.